

PROMINENCE THREAD SEISMOLOGY USING THE $P_1/2P_2$ RATIO

A. J. DÍAZ, R. OLIVER, AND J. L. BALLESTER

Departament de Física, Universitat de les Illes Balears, E-07122 Palma, Spain; toni.diaz@uib.es, ramon.oliver@uib.es, dfsjlb0@uib.es
Received 2010 June 29; accepted 2010 October 7; published 2010 December 1

ABSTRACT

Prominence threads are expected to be cold plasma condensations in a long magnetic tube. Because of this density inhomogeneity along the magnetic field, the ratio of the fundamental transverse mode period to twice that of its first overtone, $P_1/2P_2$, must differ from 1. We investigate the dependence of this ratio on the equilibrium parameters of prominence threads and its possible use as a diagnostic tool for prominence seismology. Using the low-beta plasma approximation, we follow the procedure of previous works to obtain the frequencies and spatial distribution of the modes. We also check the thin tube approximation and find it reasonably accurate. The period ratio $P_1/2P_2$ is found to be greater than unity, in contrast with coronal loops, for which the effect of inhomogeneities is to make this ratio smaller than 1. The ratio is very sensitive to the thread length, while the dependence on other parameters is less important for threads than for coronal loops. Hence, the period ratio can be used to obtain an estimation of the length of the supporting magnetic tube, since the thread length is known from observations. The obtained value of the tube length does not depend on other parameters, so their potential for prominence seismology may be great.

Key words: Sun: corona – Sun: filaments, prominences – Sun: oscillations

1. INTRODUCTION

Prominences or filaments are basically clouds of dense and cold plasma located in the corona. The magnetic field seems to be responsible for sustaining the dense material against gravity and for thermally isolating it from the surrounding hot coronal material. However, there is no clear picture of their equilibrium, creation, and eruption or disappearance, since their dynamics is quite complex and it is difficult to measure certain parameters (such as the magnetic field strength or its orientation).

These objects are known to be composed of many small thread-like structures, named fibrils or threads, which are piled up to form the body of the prominence. High-resolution observations in absorption in the $H\alpha$ line have clearly shown the existence of these structures, whose thickness seems to be less than $0\prime.3$ (and could be even lower, because of the limited spatial resolution), while their lengths are on the order of 1000–10000 km. Flows are also present in threads with velocities of 10–40 km s⁻¹ (Lin et al. 2003, 2005, 2007, 2009; Okamoto et al. 2007; Ning et al. 2009), and the dense region seems to be moving at the same time the oscillations are displayed (Lin et al. 2007, 2009; Okamoto et al. 2007; Ning et al. 2009).

There are many reports of oscillatory behavior in prominence threads (see Oliver 2009; Mackay et al. 2010 for recent summaries of observational and theoretical works). Here we concentrate on the transverse thread oscillations. Very recently, Lin et al. (2009) and Ning et al. (2009) have reported both using the Swedish Solar Telescope (SST) in La Palma and instruments on board the *Hinode* satellite that threads oscillate independently. Reported periods are around 5 minutes, while drifts and flows are sometimes seen together with the oscillatory behavior, and clear signs of damping (Arregui & Ballester 2010). These oscillations are consistent with trapped fast magnetohydrodynamic (MHD) modes of the thread (Joarder et al. 1997; Díaz et al. 2001, 2002, 2005; Díaz & Roberts 2006a; Terradas et al. 2008).

Therefore, it is suggested that the reported periods from observations could be used to perform prominence seismology and to estimate the value of equilibrium quantities, such as

the magnetic field strength or the plasma density (Díaz 2004; Terradas et al. 2008; Oliver 2009; Lin et al. 2009; Soler et al. 2010). However, the available information is not enough to obtain each unknown parameter, so some assumptions need to be made, such as choosing an ad hoc value for the prominence density. The situation does not improve if the information about the wave attenuation is taken into account, since the dissipation mechanisms require extra parameters; for example, resonant absorption needs a measure of the thread transitional layer thickness, thus adding another unknown parameter (Arregui et al. 2008; Soler et al. 2010). Moreover, the frequency of the transverse fundamental mode depends at least on the thread length, its thickness, and its density contrast with the surrounding atmosphere (Díaz et al. 2002). At best, after some assumptions on these parameters we can obtain the dimensionless ratio $\omega L/c_{Ac}$, with L being the length of the magnetic tube and $c_{Ac} = B_0/\sqrt{\mu\rho_c}$ the value for the Alfvén speed in the corona, but to obtain a value of the magnetic field we need more information about the tube length and the plasma density. Following Díaz et al. (2002), we take for example the observations in Lin et al. (2007) who report periods around 5 minutes. In the simple slab-like thread model, the normalized frequency $\omega L/c_{Ac}$ depends only on three parameters: the prominence–corona density ratio, ρ_p/ρ_c , the ratio of the thread length to the magnetic tube length, W/L , and very slightly on the ratio of the thread thickness to the magnetic tube length, a/L (since it is a small number). However, to obtain an estimated period value we need two more parameters, the Alfvén velocity in the corona or prominence (which involves the magnetic field and the density) and the tube length L . Using the values $L \approx 10^5$ km and $\rho_c \approx 10^{-12}$ kg m⁻³ (in the expected range for prominences) we obtain a value of $B_0 \approx 10$ G, which is again in the expected range, supporting the claim that these oscillations are fast MHD modes.

On the other hand, the ratio of the fundamental mode period to twice that of its first overtone, $P_1/2P_2$, has proved useful in coronal loop seismology, since it depends mainly on the density structure along magnetic field lines (see Andries et al. 2009b for a review on the topic). The first overtone itself

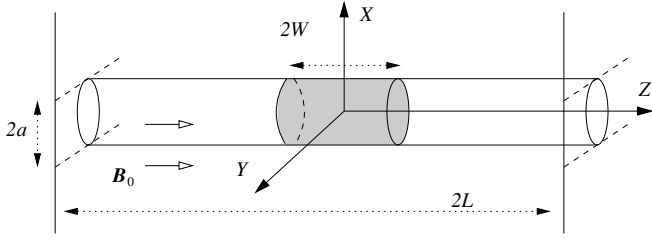


Figure 1. Sketch of a simple equilibrium configuration for prominence threads.

presents the same difficulties as the fundamental mode: too many unknown parameters, but taking the ratio $P_1/2P_2$ many of these parameters cancel out, and only the structure along the field has an impact for a thin structure, so it is a direct probe of the density scale length (since the loop length can be crudely obtained from observations). The reason for this dependence is that the first overtone has shorter scales, and it is more sensitive to variations along the field line than the fundamental mode. It is interesting to note that only in an unbounded homogeneous loop the ratio is equal to 1, since the boundaries (and finite width) lower it.

Regarding prominence threads, the ratio $P_1/2P_2$ must deviate from unity too, since they have a strong inhomogeneity along their supporting field lines. Hence, our aim is to study this dependence and to check whether similar studies can be performed in prominence seismology, despite the second period not clearly being reported yet in any observations so far.

2. EQUILIBRIUM AND NORMAL MODES

We consider a zero- β plasma embedded in a uniform magnetic field $\mathbf{B} = B_0 \hat{z}$. The plasma density outside the magnetic tube that contains the thread (with radius a) is a constant ρ_c , while inside the tube the density jumps to ρ_p for $-W \leq z \leq W$ and is equal to ρ_c in the rest of the tube, modeling the density enhancement of the thread in the central region (see also Figure 1):

$$\rho_0(r, z) = \begin{cases} \rho_p, & |z| \leq W \text{ and } r \leq a, \\ \rho_c, & r \geq a \text{ or } W < |z| \leq L. \end{cases} \quad (1)$$

Note that the Alfvén speed, termed $c_{Aj} = B_0/\sqrt{\mu_0 \rho_j}$ with $j = p, c$, is constant in each region.

The main difference of this equilibrium with that of coronal loops is that here the density enhancement is located in a small region near the top of the tube (the center of our domain), while in loops the enhancement is near the footpoints (modeling the density stratification due to gravity or the lower and denser layers of the solar atmosphere). This will become important in the ratio $P_1/2P_2$.

To obtain solutions for an arbitrary radius, we follow the same procedure detailed in Díaz et al. (2002, 2005). The boundary conditions can be satisfied if we expand the general solution as sums of the eigenfunctions in the z -direction. This leads to a system of equations for the coefficients of each eigenfunction, so the condition to have solutions different from the trivial one is that the determinant of the system vanishes and this provides us with a dispersion relation. This infinite-order determinant is then truncated so its roots can be found by using numerical algorithms.

On the other hand, Dymova & Ruderman (2005, 2006) have shown that in the thin tube limit for non-axisymmetric kink

oscillations the radial velocity, $v_r e^{i\omega t}$, satisfies an equation of the form

$$\frac{d^2 v_r}{dz^2} + \frac{\omega^2}{c_k^2(z)} v_r = 0, \quad (2)$$

where

$$c_k(z) = \left[\frac{2B_0^2}{\mu_0 [\rho_i(z) + \rho_e(z)]} \right]^{1/2} \quad (3)$$

denotes the kink speed in a tube with internal plasma density $\rho_0(z) = \rho_i(z)$ for $r \leq a$ and environment density $\rho_e(z)$ for $r > a$. In our model, the kink speed is only different from c_{Ac} inside the region filled with dense plasma

$$c_{kp}^2 = \frac{2B_0^2}{\mu_0(\rho_p + \rho_c)} = c_{Ac}^2 \frac{2}{\rho_p/\rho_c + 1}. \quad (4)$$

The thin tube equation (Equation (2)) is amenable to an analytical treatment. This method has the advantage of simplifying substantially the calculations but ignores the radial dependence and other features, such as the appearance of cutoffs and leakage. In the piecewise-constant profile we are dealing with, the thin tube approximation can be used to obtain algebraic equations for the frequencies of the modes (Dymova & Ruderman 2005; Terradas et al. 2008). In our variables, these equations are

$$f \tan[f\tilde{\omega}W/L] - \cot[\tilde{\omega}(1 - W/L)] = 0, \quad (5)$$

$$f \cot[\tilde{\omega}W/L] - \cot[\tilde{\omega}(1 - W/L)] = 0, \quad (6)$$

for the even and odd modes in the longitudinal direction, respectively. We have used the dimensionless frequency $\tilde{\omega} = \omega L/c_{Ac}$ and the definition

$$f = \sqrt{\frac{\rho_p/\rho_c + 1}{2}}. \quad (7)$$

It is also important to discuss briefly the spatial shape of these modes. The fundamental mode, i.e., the lowest frequency solution to Equation (5), has a maximum at the center (in the region filled with dense material), while the first overtone, i.e., the lowest frequency solution to Equation (6), has a zero in the center and two extrema, which can be inside or outside the dense region depending on the values of the parameters (see Figure 2). This makes the first overtone more difficult to detect, since perturbations inside the thread take small values.

3. VALIDITY OF THE THIN TUBE APPROXIMATION

We first draw the dispersion relation for typical prominence parameters, as it is shown in Figure 3 (kink modes only). We can also see that the frequencies of both the fundamental mode (an even mode) and the first overtone (which is an odd mode) are close to the cutoff frequencies when W/L is very small, but then they decrease as W/L is increased. We obtain that the thin tube limit (Equation (2)) gives us reasonable values for the frequencies of the modes.

Next, we consider the dependence of $P_1/2P_2$ on the thread thickness a (Figure 4). The curve is almost flat for values below $a/L = 0.01$, which is of the order of the expected value for threads. This result confirms that the thin tube approximation can be used with little loss of accuracy. The shape of the curve (with a minimum as a/L is increased) is caused by the dispersion of kink modes, as it was explained for coronal loops in McEwan et al. (2006; Figures 2 and 3). Since the dispersion relation for

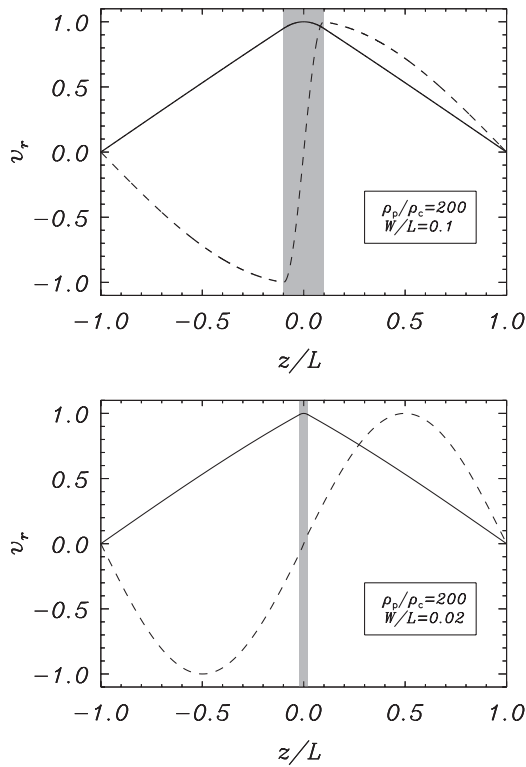


Figure 2. Cuts of v_r as a function of the normalized position along the tube z/L at the tube surface $r = a$ for two different values of W/L . Solid lines represent the fundamental mode (which is an even mode in the z -direction), while dashed lines correspond to the first overtone (which is an odd mode). The region with prominence material has been shaded.

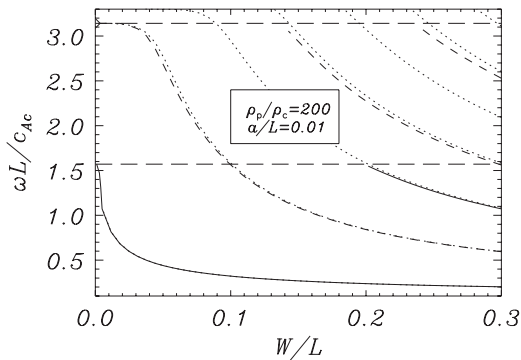


Figure 3. Dispersion diagram showing $\omega L/c_{Ac}$ against the thread length W/L for the values $\rho_p/\rho_c = 200$ and $a/L = 0.01$. Only kink modes are shown. Solid lines correspond to even modes about the middle point of the tube, while dashed lines correspond to odd modes. The results of the thin tube approximation (Equation (2)) have been overplotted in dotted lines. The horizontal dashed lines represent the two cutoff frequencies of the system, one for the even modes ($\omega L/c_{Ac} = \pi/2$) and one for the odd modes ($\omega L/c_{Ac} = \pi$).

prominence threads has a similar mathematical form (Díaz et al. 2002) using the thread thickness the curve resembles those plots. Plotting similar curves for different values of W/L and ρ_p/ρ_c would only change the value at the origin, with the shape of the curve very similar to that in Figure 4.

Our next parameter is the density contrast between the prominence and coronal material, ρ_p/ρ_c . We can see in Figure 5 that the curve is close to flatness for density ratios over 100, which is the expected range for the prominence material in threads. This is important, since both the coronal and the prominence densities are difficult to measure simultaneously with the oscillatory properties of the structure, but we can see that it is not a crucial

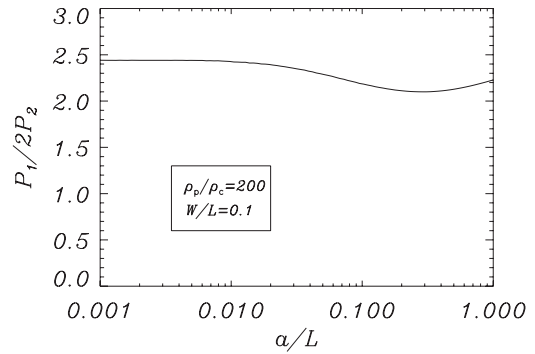


Figure 4. Ratio $P_1/2P_2$ against the thread radius for the values $\rho_p/\rho_c = 200$ and $W/L = 0.1$.

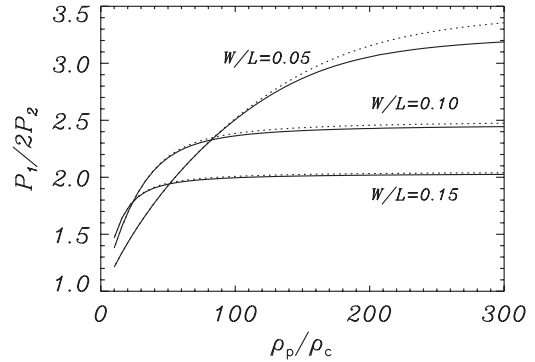


Figure 5. Ratio $P_1/2P_2$ against the density ratio for a radius $a/L = 0.01$ and different values of W/L . The results from the thin tube approximation have been overplotted as a dotted line.

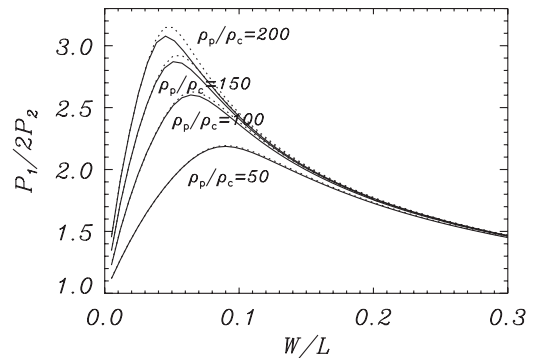


Figure 6. Ratio $P_1/2P_2$ against the thread length for a radius $a/L = 0.01$ and different values of ρ_p/ρ_c . The results from the thin tube approximation have been overplotted as a dotted line.

parameter, and thus our parameter space is reduced. Again we check that the thin tube limit gives reasonable results, although for low values of the thread length, W , it is less accurate.

Finally, we study the effect of the thread length, W , shown in Figure 6. First of all, the dependence is quite more important and the period ratio shows variations up to a factor of three, while as W/L tends to 1 (so the whole tube is filled with dense material) the ratio tends to a value slightly less than 1 because of the finite value of the thread thickness used (this is not shown in the plot).

It is also important to note that the curve is multivaluated: for a given value of the period ratio, there are two possible values of the thread length. This is caused by the first overtone becoming a mode with amplitude mainly on the evacuated part of the loop, with its frequency very close to π (and a sinusoidal shape) and not sensitive to the amount of dense material near the center, while the fundamental mode is still affected by this material.

This transition can be seen in Figure 2: in the top panel (W/L in the expected range) both modes are affected by the dense material; on the other hand, in the bottom panel (W/L small) the second overtone is very close to a sinusoidal form, while the fundamental mode still reflects the prominence material and its far from a sinusoidal form.

4. ANALYTICAL APPROXIMATIONS TO $P_1/2P_2$

4.1. Series Expansion for Small Frequencies

The relations in Equations (5) and (6) can be used to obtain a series expansion and a simple approximated formula for $P_1/2P_2$. If we assume that $\tilde{\omega}$ is less than unity, we can use the series expansion of the trigonometric functions and obtain analytical approximations from these transcendental equations:

$$\begin{aligned} \tilde{\omega}_1 &\approx [(1 - W/L)(W/Lf^2 - W/3L - 1/3)]^{-1/2}, \\ \tilde{\omega}_2 &\approx [W/L(1 - W/L)(W/Lf^2 - W/L - 1)/3]^{-1/2}. \end{aligned} \quad (8)$$

Then, the period ratio turns out to be

$$P_1/2P_2 \approx \frac{1}{2\sqrt{W/L}} \sqrt{\frac{1 + W/L(3f^2 - 1)}{1 + W/L(f^2 - 1)}}. \quad (9)$$

We can further simplify these expressions if we assume that the density ratio ρ_p/ρ_c is much bigger than unity, so $f \gg 1$ and these expressions give

$$\begin{aligned} \tilde{\omega}_1 &\approx [W/L(1 - W/L)]^{-1/2}/f, \\ \tilde{\omega}_2 &\approx 3^{1/2}[(W/L)^2(1 - W/L)]^{-1/2}/f. \end{aligned} \quad (10)$$

Hence,

$$P_1/2P_2 \approx \sqrt{\frac{3}{4W/L}}, \quad (11)$$

which does not depend on the density ratio showing that the dependence on this parameter is not crucial.

Note however that this expansion is only valid when the frequencies are small compared with $\pi/2$. We can see in Figure 3 that the fundamental mode satisfies this condition except for small W/L , but the first overtone does not, and hence the approximation is quite poor. We can compute similar formulae adding an extra term in the expansion of the trigonometric functions in Equations (5) and (6) and then using again $f \gg 1$, obtaining the next order correction:

$$P_1/2P_2 \approx \sqrt{\frac{3}{4W/L}} \sqrt{\frac{1 + \sqrt{(1 + W/L/3)/(1 - W/L)}}{1 + \sqrt{(9/5 - W/L)/(1 - W/L)}}}. \quad (12)$$

4.2. Series Expansion for Small Thread Length

The formulae in the previous subsection are valid only if the frequency is small $\tilde{\omega} \ll \pi/2$. However, we see in Figure 3 that for small values of the thread length W/L this assumption is no longer valid. Instead, in this range the frequencies are close to the cutoff frequencies, so this suggests using their values as the center of the expansions in Equations (5) and (6). Then we use another series expansion for $W/L \ll 1$ to obtain the following expressions:

$$\begin{aligned} \tilde{\omega}_1 &\approx \frac{\pi}{2} \frac{4 + \pi^2(W/L)^2}{8 + 2W/L(\pi^2(W/L)^2 + 4W/L(f^2 - 1) + 4)}, \\ \tilde{\omega}_2 &\approx \pi \frac{3 + \pi^2(W/L)^2}{3 + \pi^2(W/L)^2(1 + W/L(f^2 - 1))}. \end{aligned} \quad (13)$$

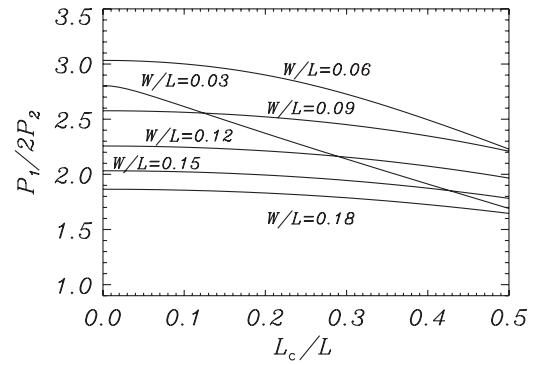


Figure 7. Ratio $P_1/2P_2$ against the thread center position L_c for a density contrast $\rho_p/\rho_c = 200$ and different values of the thread width W/L (thin tube approximation).

Then, the period ratio gives

$$P_1/2P_2 \approx 1 + (f^2 - 2)W/L - (f^2 + 1)(W/L)^2. \quad (14)$$

In this range there is a dependence on the density ratio, as we expected from the curves in Figure 6. However, the range where this formula can be applied is small, since the fundamental mode differs rapidly from $\pi/2$ as W/L is increased, so the condition for the expansion is no longer met and the curve of $P_1/2P_2$ reaches the maximum in Figure 6, with the decrease after the maximum reasonably described by the approximations in the previous subsection (Equation (12)).

5. DEPENDENCE OF THE PERIOD RATIO ON THE THREAD POSITION ALONG THE MAGNETIC STRUCTURE

So far we have dealt with threads which are positioned in the center of the magnetic structure (Figure 1). However, in a solar prominence this is not necessarily true, so we explore the dependence of the ratio on the thread position. We define L_c as the position of the center of the thread with respect to the center of the structure (which is situated at $z = 0$), so $|L_c| \leq L - W$. Hence, the density along the magnetic structure is ρ_p if $L_c - W \leq z \leq L_c + W$ and ρ_c otherwise, instead of the profile in Equation (1).

Using both the thin tube approximation and the numerical code we can obtain the eigenmodes for different values of this new parameter. The results of the numerical code are shown in Figure 7.

There are two types of behavior for these curves: either a slight dependence on L_c or a definite drop. This can be related with the two regimes that appear in Figure 6: if the value of W/L is smaller than the position of the maximum, then the ratio is highly dependent on the position of the thread; however, if the value of W/L is greater than the position of the maximum then the value of the period ratio is only slightly modified when L_c is changed. These two different shapes of the $P_1/2P_2$ curve can be explained looking at the spatial shape of the modes (Figure 2). For high values of W/L the mode amplitude is higher in the dense region, and moving it does not affect too much the shape (and period) of the modes. On the other hand, for lower values of W/L the amplitude of the first overtone peaks outside the dense region, and moving it distorts its shape (it is no longer quasi-sinusoidal), changing significantly its period and hence the period ratio.

Therefore, the effect of modifying the thread position along the magnetic structure is only important for small thread lengths

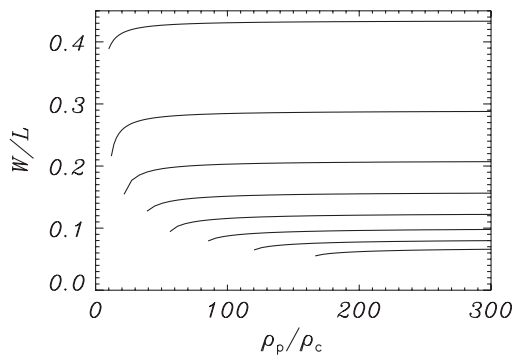


Figure 8. Plots of the lines satisfying $P_1/2P_2 = \text{constant}$ in the space parameter. The upper line corresponds to $P_1/2P_2 = 1.25$ and the lower one $P_1/2P_2 = 3$, with each line showing an increment of 0.25 from the previous one.

(smaller than the position of the maximum in Figure 6), so the series in Section 4.2 are only valid for $L_c < W$. On the other hand, the results for larger thread lengths are accurate enough if this effect is not considered.

6. THE $P_1/2P_2$ PERIOD RATIO AS A SEISMOLOGICAL TOOL

One of the main problems in prominence and coronal seismology is that normally there are too many parameters on which the frequency depends, and hence, it is difficult to extract information from the observation without making assumptions on the values of unknown quantities. However, the situation is a bit different if we consider the period ratio, since all the dependence on the dimensionless frequency is canceled, leaving only the dependence on the parameters that describe the inhomogeneity along the field lines (McEwan et al. 2008). Since the thread thickness is small we are only left with two parameters: ρ_p/ρ_c and W/L . The dependence of the period ratio on these parameters is shown in Figure 8. Note that the dependence on the thread density ratio is very small; the curves are almost flat. Also not all the values can be reached: if the density becomes too small a big value of $P_1/2P_2$ might not be reached.

Hence, we can see the potential use of this seismological tool: given the period ratio from an observation, it only depends on W/L in first approximation. This is plotted in Figure 9, where the results of the series expansion have been overplotted. These analytical formulae may be helpful, but the lack of accuracy must be noticed. Using a simple expression such as Equation (11) may be interesting theoretically, but for higher precision the numerical solution must be used.

Finally, once W/L has been obtained we can estimate the value of the magnetic field tube length, L , since the thread length W can be determined quite accurately from the observations. Moreover, the deduced tube length could be compared with coronal magnetic field extrapolations and Michelson Doppler Imager (MDI) photospheric magnetograms to test the validity of our models and the structure of the prominence supporting magnetic field.

The second period has not been unambiguously reported so far, but there seem to be hints of it in some observations. As an example, consider the results in Lin et al. (2007), where two periods are present in their observations of a prominence region, namely, $P_1 = 16$ minutes and $P_2 = 3.6$ minutes. Although the identification of these periods with the fundamental mode and its first overtone is not clear, let us assume that this was a detection of these modes. Inverting the data of Figure 9, we obtain for the observed period ratio the value $W/L = 0.12$. It is difficult to

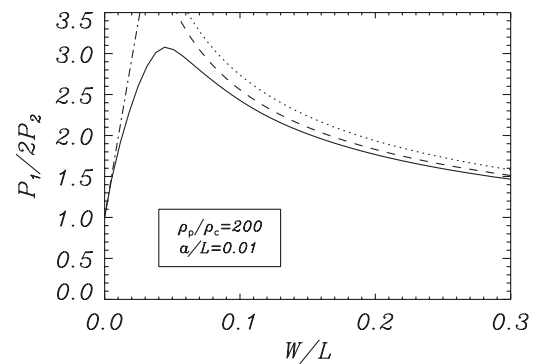


Figure 9. Ratio $P_1/2P_2$ against the thread length for a radius $a/L = 0.01$ and a density contrast $\rho_p/\rho_c = 200$. The results from the thin tube series approximation have been overplotted as a dotted line (Equation (11)), dashed line (Equation (12)), and dot-dashed line (Equation (14)).

estimate the length of this particular thread, W , from the data reported in the paper, but if we assume that it is about 18'' (as for other threads studied in the paper), this would give an approximate length $W \approx 13,000$ km, and hence a tube length $L \approx 110,000$ km, which is consistent with the expected range of this parameter.

Finally, we can use this new seismological information to obtain more values, namely, the Alfvén speed in the prominence. Rearranging Equation (10), using Equation (4), and assuming that $\rho_p \gg \rho_c$ we find an expression for c_{Ap} which depends only on known quantities, namely,

$$c_{Ap} = \frac{\pi L}{P_1} \sqrt{2W/L (1 - W/L)}. \quad (15)$$

Finally, we perform this calculation with the observational data, which give us an estimated value of $c_{Ap} \approx 160$ km s⁻¹.

7. DISCUSSION AND CONCLUSIONS

We have tested the thin tube approximation in Dymova & Ruderman (2005) and have found that its results are quite accurate. Then, we have explored the dependence of the $P_1/2P_2$ ratio on the plasma parameters and equilibrium configuration. First of all, the ratio does not depend on unknown quantities such as the magnetic field or the coronal density (since the dependence on the Alfvén speed is canceled). Moreover, the dependence on the thread thickness is negligible, while the dependence on the density ratio between the prominence and the surrounding corona turns out to be small for typical prominence values. This is caused by the large inertia of the prominence material filling the central part of the magnetic tube compared to that of the coronal plasma in the evacuated part of the tube. If the density contrast is lower then its effect on the ratio must be taken into account too.

Hence, we are left with only one important parameter: the thread length over the magnetic field line length W/L , whose influence on the period ratio can be seen in Figure 9; we have also derived analytical approximations to this curve (Equation (11)). The reason why this parameter is so important is because it controls how the structure deviates from a homogeneous tube. However, there is a maximum value of the ratio in this figure, and then it decreases as W/L is further decreased. The reason for this shape is that for tubes with a small dense region the first overtone no longer feels it and becomes almost a mode of the field line itself. In this case we have shown that deviations of the thread position from the center of the field line may also

modify significantly the period ratio, otherwise this ratio is not too sensitive to the position of the thread, provided it is not too close to the footpoints.

These results would allow us to perform prominence thread seismology. A reported value of $P_1/2P_2$ would allow us to deduce a value of W/L , so once the actual length of the thread is determined from the observations the length of the magnetic field line L could be deduced. The problem of multivaluation in Figure 9 is still present, but some information about the structure around the body of the prominence (such as surface magnetograms) could help to rule out spurious values. Once the value of the tube length L has been deduced, the local Alfvén speed can be obtained from the actual value of P_1 (Díaz et al. 2002, assuming that the density ratio is large) or with less precision with formulae from the series expansion (Equation (15)), since P_1 depends slightly on this parameter too. To obtain a value for the magnetic field strength B_0 we need to know also the prominence plasma density ρ_p , but the determination of W/L does not rely on unknown quantities, and it can be a useful tool to help understand the complex magnetic field that is the backbone of a prominence. The seismological information that can be obtained from the P_1 period alone is less precise; for example, in Terradas et al. (2008) the ranges of the equilibrium quantities consistent with a given observation were determined, while the ratio $P_1/2P_2$ leads to a straight determination of some of these parameters (especially L and c_{Ap}).

Regarding the observations, no measurement of the first overtone period, P_2 , has been reported in the literature so far for prominence threads, although there seems to be plenty of periods and overtones when the prominence is observed as a whole (see, for example, Pouget et al. 2006). The period of the fundamental mode in prominence threads is around 5 minutes (Lin et al. 2003, 2009), so for a typical set of values of the parameters the first overtone period would be around 2 minutes, which is close to the cadence of some instruments but can still be observed with others. It is possible that this second period is already present in more data sets, but has not been reported so far. On the other hand, this overtone is an antisymmetric mode with a node in the center of the dense region, so probably it is difficult to detect near the thread center and easier to detect near its edges. It must be mentioned that in Lin et al. (2007) a second peak in the power spectrum is found, but the authors suggest that it could be the fundamental mode of a overlaying thread; however, it could also be a spurious peak from the data analysis.

There are further additions to the model presented in this work. First of all, field divergence is an important factor in coronal loop seismology using $P_1/2P_2$ since it competes with density structuring (Verth & Erdélyi 2008), but since its main contribution is to rise a few % in prominence threads the effect can be neglected, the density structuring being much stronger and already raising the ratio. It is also known that flows are present in threads (Lin et al. 2003, 2005, 2007, 2009). However, the effect on the periods is small, since these flows are generally small compared with the local Alfvén speed (Terradas et al. 2008; Soler et al. 2009), and hence its effect on the ratio should also be small. More important deviations could come from different equilibrium configurations, such as threads having the dense part not centered in a field line (which we have seen that is important for thin threads) or more than one dense part in the same field line.

We have so far considered the ratio of the fundamental mode period to twice that of its first overtone, $P_1/2P_2$, but a similar

study could be performed on the ratio of the fundamental mode to three times that of its second overtone, $P_1/3P_3$, and its deviation from unity. In principle, the second overtone is again an even mode, so it is easier to detect, and $P_1/3P_3$ would give similar results to the ones with $P_1/2P_2$. However, leakage turns out to be an important factor. We see in Figure 3 that very few modes are trapped. The rest of the modes are leaky (their frequencies lie above the cutoff frequencies) and thus radiate energy away from the structure. These leaky modes only appear during the short transients at the moment of excitation and are difficult to detect. We can also see that both the fundamental mode (an even mode) and the first overtone (which is an odd mode) are present in the whole range, while higher overtones become leaky when the thread length is decreased. Hence, it makes sense to compute the $P_1/2P_2$ diagram, while similar diagrams for higher overtones would reach an end when the overtone becomes leaky and would provide little information in the expected range of W/L . One should realize that in the thin tube limit one can obtain a value for all the range of parameters, but this limit does not take into account that overtones may become leaky.

It is also interesting to remark that the value of $P_1/2P_2$ is above unity. This is opposite to its behavior in coronal loops: for such systems the density structuring was found to lower the value of this ratio (Andries et al. 2005, 2009a; McEwan et al. 2006, 2008; Goossens et al. 2006; Díaz & Roberts 2006b; Erdélyi & Verth 2007; Verth et al. 2008; Morton & Erdélyi 2009), except if other effects are taken into account, such as the divergence of the field lines that form the tube (Verth & Erdélyi 2008). However, in the thread equilibrium the density acts raising the ratio, and the reason is that now we have denser material on the tube center, while for coronal loops the plasma is denser near the footpoints. Also note that the ratio deviates less than 20% from unity for coronal loops, but in prominence threads the deviation is larger than 100%, since we have a clear deviation from a homogenous loop. The effect of the magnetic field is then less relevant, since it would increase a little this ratio, but since it is already well above 1 the effect would be less important than for coronal loops, for which it balances the deviations due to structuring.

A.J.D. thanks the Spanish MICINN for support under a Juan de la Cierva Postdoc Grant. A.J.D., R.O., and J.L.B. also acknowledge the financial support received from the Spanish MICINN and FEDER funds, under grant No. AYA2006-07637. J.L.B. acknowledges discussions within ISSI Team on Solar Prominence Formation and Equilibrium: New data, New models. The authors also thank B. Roberts for useful suggestions and comments.

REFERENCES

- Andries, J., Arregui, I., & Goossens, M. 2005, *ApJ*, 624, L57
 Andries, J., Arregui, I., & Goossens, M. 2009a, *A&A*, 497, 265
 Andries, J., van Doorsselaere, T., Roberts, B., Verth, G., Verwichte, E., & Erdélyi, R. 2009b, *Space Sci. Rev.*, 149, 3
 Arregui, I., & Ballester, J. L. 2010, *Space Sci. Rev.*, 59
 Arregui, I., Terradas, J., Oliver, R., & Ballester, J. L. 2008, *ApJ*, 682, L141
 Díaz, A. J. 2004, PhD thesis, Universitat de les Illes Balears, Palma Mallorca
 Díaz, A. J., Oliver, R., & Ballester, J. L. 2002, *ApJ*, 580, 550
 Díaz, A. J., Oliver, R., & Ballester, J. L. 2005, *A&A*, 440, 1167
 Díaz, A. J., Oliver, R., Erdélyi, R., & Ballester, J. L. 2001, *A&A*, 379, 1083
 Díaz, A. J., & Roberts, B. 2006a, *Sol. Phys.*, 236, 111
 Díaz, A. J., & Roberts, B. 2006b, *A&A*, 458, 975
 Dymova, M. V., & Ruderman, M. S. 2005, *Sol. Phys.*, 229, 79
 Dymova, M. V., & Ruderman, M. S. 2006, *A&A*, 457, 1059

- Erdélyi, R., & Verth, G. 2007, *A&A*, **462**, 743
- Goossens, M., Andries, J., & Arregui, I. 2006, *Phil. Trans. R. Soc. Ser. A*, **364**, 433
- Joarder, P. S., Nakariakov, V. M., & Roberts, B. 1997, *Sol. Phys.*, **176**, 285
- Lin, Y., Engvold, O., Rouppe van der Voort, L. H. M., & van Noort, M. 2007, *Sol. Phys.*, **246**, 65
- Lin, Y., Engvold, O., Rouppe van der Voort, L., Wiik, J. E., & Berger, T. E. 2005, *Sol. Phys.*, **226**, 239
- Lin, Y., Engvold, O. R., & Wiik, J. E. 2003, *Sol. Phys.*, **216**, 109
- Lin, Y., Soler, R., Engvold, O., Ballester, J. L., Langangen, Ø., Oliver, R., & Rouppe van der Voort, L. H. M. 2009, *ApJ*, **704**, 870
- Mackay, D. H., Karpen, J. T., Ballester, J. L., Schmieder, B., & Aulanier, G. 2010, *Space Sci. Rev.*, **151**, 333
- McEwan, M. P., Díaz, A. J., & Roberts, B. 2008, *A&A*, **481**, 819
- McEwan, M. P., Donnelly, G. R., Díaz, A. J., & Roberts, B. 2006, *A&A*, **460**, 893
- Morton, R. J., & Erdélyi, R. 2009, *A&A*, **502**, 315
- Ning, Z., Cao, W., Okamoto, T. J., Ichimoto, K., & Qu, Z. Q. 2009, *A&A*, **499**, 595
- Okamoto, T. J., et al. 2007, *Science*, **318**, 1577
- Oliver, R. 2009, *Space Sci. Rev.*, **149**, 175
- Pouget, G., Bocchialini, K., & Solomon, J. 2006, *A&A*, **450**, 1189
- Soler, R., Arregui, I., Oliver, R., & Ballester, J. 2010, *ApJ*, **722**, 1778
- Soler, R., Oliver, R., & Ballester, J. L. 2009, *ApJ*, **693**, 1601
- Terradas, J., Arregui, I., Oliver, R., & Ballester, J. L. 2008, *ApJ*, **678**, L153
- Verth, G., & Erdélyi, R. 2008, *A&A*, **486**, 1015
- Verth, G., Erdélyi, R., & Jess, D. B. 2008, *ApJ*, **687**, L45